ELSEVIER

Chemical Engineering Journal 71 (1998) 77–85

Chemical Engineering Journal

Implementing operating trajectories in an exothermic chemical batch reactor by a self-tuning single neuron controller

Jyh-Shyong Chang*, Yie-Jane Liu

Department of Chemical Engineering, Tatung Institute of Technology, Taipei, Taiwan

Received 20 October 1997; received in revised form 13 May 1998; accepted 1 June 1998

Abstract

A self-tuning single neuron controller was developed and applied to track operating trajectories in an exothermic chemical batch reactor. By self-tuning only the slope of the non-linear saturated function b, the adopted single neuron controller can track a given operating trajectory closely by merely observing the process output error. Experimental results reveal the applicability of such a self-tuning single neuron controller for tracking a given trajectory in batch reactors.

Keywords: Trajectory tracking; Batch reactor; Control

1. Introduction

There is considerable interest in tracking a given operating trajectory for batch chemical reactors [1,2]. Usually, a batch reactor system can be represented by

$$\dot{\boldsymbol{x}} = \boldsymbol{f}(\boldsymbol{x}, u) \quad y = h(\boldsymbol{x}) \tag{1}$$

The objective is to find a control law so that $y(t)$ tracks a given trajectory $y^*(t)$. In essence, the appropriate choice of a set-point policy and a suitable controller for trajectory tracking pave the way for the operation of a batch reactor. Many studies have proposed control strategies in dealing with the trajectory tracking problem of batch reactors [1,3]. Previous studies [4–7] have dealt with the trajectory tracking problem by proposing a model-based control law. The performance of the model-based control law is predictable if the model identified reflects the actual behaviour of the process suitably. However, the development of a reliable model is usually time consuming and can be unfeasible in practice. Therefore, it is rewarding to adopt a model-free control law as an alternative to tackle the trajectory tracking problem.

Chen and Chang [8] developed an autotuning neural controller designed by a single neuron. Because of its simplicity and model-free design approach, Chang et al. [9] modified this controller from three autotuning parameters into only one autotuning parameter. Although acceptable performance of this simplified single neuron controller was obtained through simulations and experiments, the term $\partial y/\partial u$, which is the derivative of the controlled output with respect to the controller output, needs to be calculated to obtain the adjusting parameter b in the controller law. This may be a disadvantage when adopting this control law, especially in the face of noisy measurements. Therefore, we extended the design concept of the single neuron controller [8,9] by devising a self-tuning single neuron controller. Our simulation studies prove the satisfactory operation of this method, and we describe the performance of the self-tuning single neuron controller in a batch reactor apparatus on the basis of the experimental results.

2. Trajectory tracking using a self-tuning single neuron controller

Chen and Chang [8] developed the following autotuning neural controller designed by a single neuron

$$u = h(e-\theta) = \frac{a'[(1-\exp(-b'(e-\theta))]}{[1+\exp(-b'(e-\theta))]} \tag{2}$$

Based on the control objective function defined at each control step

$$E(k) = \frac{1}{2}[y^*(k) - y(k)]^2 = \frac{1}{2}e^2(k) \tag{3}$$

*Corresponding author. Fax: +886-2-5861939; e-mail: jschang@che.ttit.edu.tw

1385-8947/98/$ – see front matter
PII: S1385-8947(98)00117-X

Chen and Chang [8] developed the following autotuning formula

$$\theta^{(k+1)} = \theta^{(k)} - \eta\left[\frac{1}{2}ea'b'\left(1-\frac{u}{a'}\right)\left(1+\frac{u}{a'}\right)\frac{\partial y}{\partial u}\right] \quad (4)$$

$$a'(k+1) = a'(k) + \eta\left[e\frac{u}{a'}\frac{\partial y}{\partial u}\right] \quad (5)$$

and

$$b'(k+1) = b'(k) - \eta\left[\frac{1}{2}ea'(e-\theta)\left(1-\frac{u}{a'}\right)\left(1+\frac{u}{a'}\right)\frac{\partial y}{\partial u}\right] \quad (6)$$

where e is the input error signal, θ is the threshold value, u is the output signal of the single neuron, y is the controlled output, h is the non-linear saturated function (NSF), a' is the saturated level of the NSF, b' is the slope of the NSF and η is the learning rate. Chang et al. [9] modified their control law and applied it to tackle the trajectory tracking problem considered in the experimental system given in Section 4. Because the control action u is designed to be bounded between zero and unity in the experimental system, we set the value of a' to be unity, and the value of θ (threshold value) was chosen to be the desired tracking error $(T_b^* - T_b)$. Therefore, the resulting neuron controller is only autotuned by parameter b'. The design equation of the modified single neuron controller was chosen as

$$u = h(e-\theta) = \frac{1}{[1+\exp(-b'(e-\theta))]} \quad (7)$$

Based on the control objective function defined at each control step (Eq. (3)), the following autotuning formula can be derived

$$b'(k+1) = b'(k) - \eta\left[e(e-\theta)u^2\exp(-b'(e-\theta))\frac{\partial y}{\partial u}\right] \quad (8)$$

$$0 \le b' \le b'_{\max}$$

An upper limit of b' must be chosen so that the term $\exp(-b'(e-\theta))$ will not diverge. Although acceptable performance of this simplified single neuron controller was obtained through simulations and experiments, the term $\partial y/\partial u$, which is the derivative of the controller output with respect to the controller output, needs to be calculated to obtain the adjusting parameter b' in the controller law. This may be a disadvantage when adopting this control law, especially in the face of noisy measurements. Therefore, we developed the following self-tuning single neuron controller

$$u(t) = \frac{a}{[1+\exp(-b(t)(e(t)-\theta))]} \quad (9)$$

$$e(t) = T_b^*(t) - T_b(t) \quad (10)$$

The following self-tuning formula for $b(t)$ is proposed

$$b(t) = b_{\max}\left[\frac{2}{1+\exp(-c|e(t)|)} - 1\right] \quad (11)$$

where $\theta(\cong 1\times10^{-3})$ is the threshold value used in Eq. (9) and a is the scaling factor. Based on the chosen parameter c, the self-tuning function $b(t)$ is computed on-line using $e(t)$ not $\partial y/\partial u$ and provides a variable with a numerical value sliding between $[0\rightarrow b_{\max}]$. The single neuron controller is thus devised to output a larger or smaller value of $u(t)$ depending on whether $e(t)$ is increased or decreased, by increasing or decreasing the value of $b(t)$. The degree of non-linear characteristic for $u(t)$ depends primarily on parameters c and $b_{\max}$; therefore, a suitable choice of these parameters can provide a proper tuning of $u(t)$. If the value of $b_{\max}$ is chosen too large, a quick change of $u(t)$ may degrade the performance of the self-tuning single neuron controller. Because we cannot determine parameters c and $b_{\max}$ a priori, a suitable choice of these parameters for a specific system needs to be obtained by experiment.

3. The reaction system

The reaction system considered in the experiment is the hydrolysis reaction of acetic anhydride in acetic acid. This is a strongly exothermic reaction ($\Delta H = -1.741\times10^5$ kJ kmol^{-1}) and has industrial applications. The hydrolysis reaction of acetic anhydride takes place in the manufacture of food-grade acetic acid, in cotton acetylation reactions and, as a side reaction, in the manufacture of acetic anhydride from acetaldehyde [10,11].

4. Experimental apparatus

Fig. 1 provides a schematic diagram of the experimental apparatus. The reactor is a 0.0122 m^3 (10 l) stainless steel cylindrical vessel with a 0.0254 m (1 in.) drain centred at the bottom. The vessel is composed of an annular jacket with baffling and internal helical coils. The reacting mixture is blended with an agitator (diameter, 0.22 m), at one end of which is a pitched flat-blade paddle and at the other a pitched anchor-type paddle. The rotational speed of the agitator is 120 rpm. Table 1 lists the detailed specifications of the reactor vessel.

Table 1
Specifications of reactor vessel

D_T (m) = 0.24	H (m) = 0.27
D_{imp} (m) = 0.22	N (rps) = 7.2×10^3
D_{jo} (m) = 0.26	D_{ji} (m) = 0.24
d_{co} (m) 2.13×10^{-2}	d_{ci} (m) = 1.58×10^{-2}
D_c (m) = 0.18	N_c (m) = 6
V (m) = 1.22×10^{-2}	

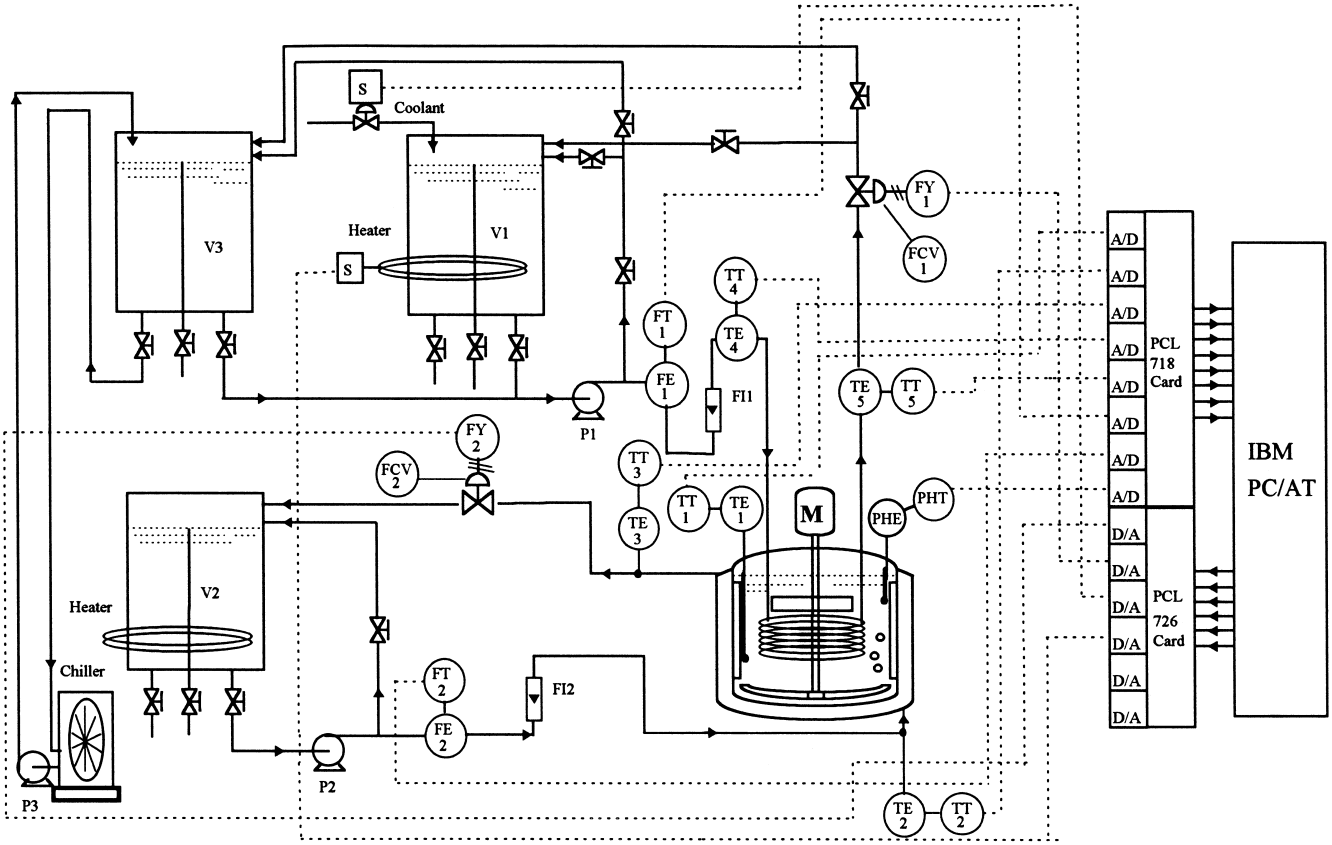

Fig. 1. Schematic diagram of the experimental apparatus.

One vessel, V1, was used to provide the coolant. Another vessel, V2, was installed to serve as the heating medium. Another vessel, V3, was used to provide a lower temperature coolant (about 8°C) than V1 by circulating the water of this vessel through a chiller. These three vessels were about 0.08 m^3 in volume. A single overflow pipe was inserted to maintain a constant head for each vessel. During the reaction, if the coolant flow rate was raised to above 10 l min^{-1}, the temperature of the water in V1 was considered to be too high and was adjusted by external cooling water using an ON/OFF solenoid valve. On the other hand, if the coolant flow rate was reduced to below 5 l min^{-1}, the temperature of the water in V1 was considered to be too low and was adjusted with an electric heater controlled by a solid-state relay (SSR). Meanwhile, the electric heater installed in V2 was also adjusted by an SSR to maintain the desired temperature of the heating medium.

Computer control and the installed instrumentation for the experimental apparatus are also shown in Fig. 1. The computer (IBM PC/AT type) was connected to a PCL-718 A/D interface card and a PCL-726 D/A interface card (both from Advantech Corp). These two interface cards used 12-bit converters; therefore, the digital signals were 12 bit. The analogue signals from the measuring elements were amplified and conditioned by AT740 (4–20 mA/0–5 V) modules (from Acel Corp.). The data acquisition software was developed by the authors.

Heating of the reaction mixture was achieved by adjusting the flow rate of hot water, F_{wj}, through the jacket side of the reactor with a 3.72 kW centrifugal pump. Heat removal was carried out by manipulating the flow rate of the coolant, F_{wc}, through the internal helical coil with another 3.72 kW centrifugal pump. Two pneumatic control valves, two flow meters and two rotameters were installed in the flow control loops. At the inlets and outlets of the jacket and the coil, four temperature sensors were located (0–120°C resistance temperature detector (RTD); accuracy, ±0.3°C). The reactor temperature was measured by an RTD of the same type (accuracy, ±0.1°C). The volumetric flow rates inside the jacket and the coil were measured by two Compak flow transmitters (MK508 and MK2350 from Signet Industrial) which output a 4–20 mA signal proportional to the flow rate.

The response of a pH meter for the same concentration of reacting medium at different temperatures varies. Therefore, in order to apply a pH meter for the monitoring of the extent of reaction correctly as the reaction proceeds, a cooling and holding system was designed and installed (Fig. 2) to provide the sensor of the pH meter with a near-isothermal reacting medium (22–24°C). As shown in Fig. 2, the reacting medium was pumped out through a stainless steel cooling coil and returned to a holding bottle. At the bottom of the holding bottle, an S-shaped tube with an upward venting tube was connected to the reactor vessel. The venting tube was installed to prevent the syphon effect

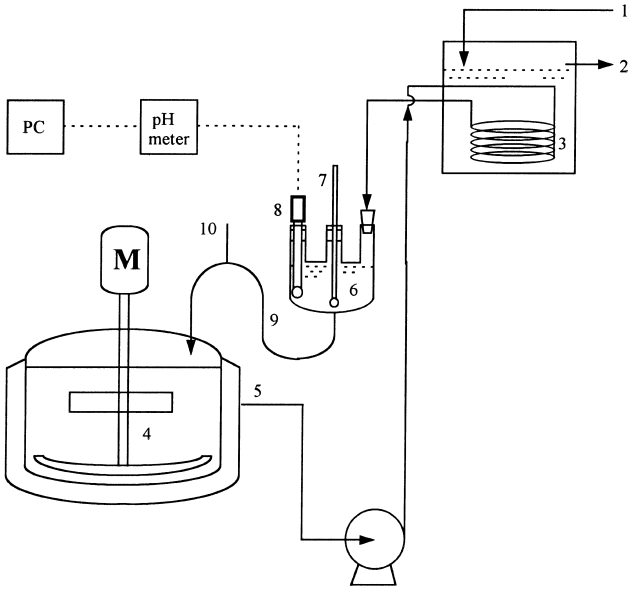

1. Coolant inlet
2. Coolant outlet
3. Surge tank
4. Reactor
5. Sample pumping out
6. Liquid holding bottle
7. Thermometer
8. Sensor of pH meter
9. S-shape tube
10. Venting line

Fig. 2. Schematic diagram of the cooling and holding apparatus for the pH sensor.

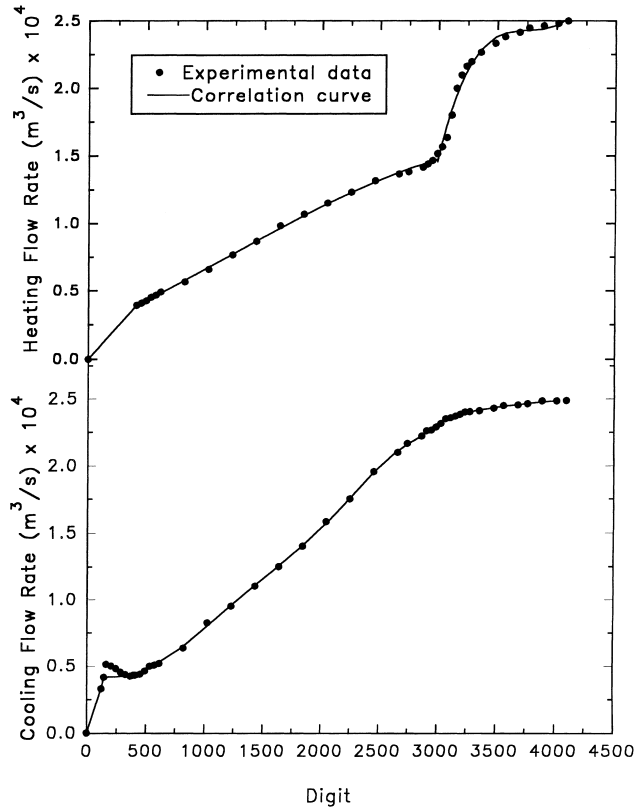

Fig. 3. Curve fittings of flow rates (F_{wj}, F_{wc}) and digital signals (D/A).

and the S-shaped tube was designed to maintain a constant liquid level in the holding bottle. In this way, the sensor of the pH meter (F-23 from Horiba; accuracy, ±0.001 pH units) would not lose its contraction with the reacting medium.

4.1. Dynamics of the control elements

Compared with the dynamics of the reactor, jacket and coil, the dynamics of the control elements (the control valve, RTD, control valve pressure transducer and heater) were very fast. The steady-state input/output behaviour of most of these elements showed that a linear relationship existed in all signals, except that between the air pressure and the flow for the two air-to-open control valves. We used the quadratic calibration equation to calculate the actual flow rate from the corresponding digital signal and vice versa (Fig. 3).

4.2. Implementation of the control law

To track a reference temperature trajectory closely in a batch reactor, both heating and cooling of the process are necessary. Therefore, the experimental apparatus (Fig. 1) was designed to meet this requirement. In order to control a single output (T_b) through two manipulated variables (F_{wj} and F_{wc}) the control system will be excessively determined. A way of solving this difficulty is to introduce a single parametric variable u [12] such that

$$F_{wj} = (F_{wj,max} - F_{wj,min})u + F_{wj,min} \quad (12)$$
$$F_{wc} = (F_{wc,min} - F_{wc,max})u + F_{wc,max}$$

Clearly, $u = 0$ represents the maximum cooling and $u = 1$ the maximum heating of the system. This parametric variable is used as a single control variable for this tracking problem. Fig. 4 shows the block diagram for the self-tuning single neuron controller and the process.

5. Experimental materials

Acetic anhydride (reagent grade) was used without any further purification. Considering the initial concentration of the acetic anhydride to be 2 kmol m^{-3}, a total of 10 l of reacting mixture (2.04 l of acetic anhydride and 7.96 l of distilled water) was loaded in the reactor for each run. Hydrolysis of acetic anhydride proceeded with or without catalyst (3% sulphuric acid). A pH meter was used to monitor the progress of hydrolysis.

6. Results and discussion

6.1. Adiabatic reaction

To demonstrate that the hydrolysis reaction is highly exothermic, Fig. 5 depicts the results of experiments carried out at an initial temperature of 30°C in the absence of

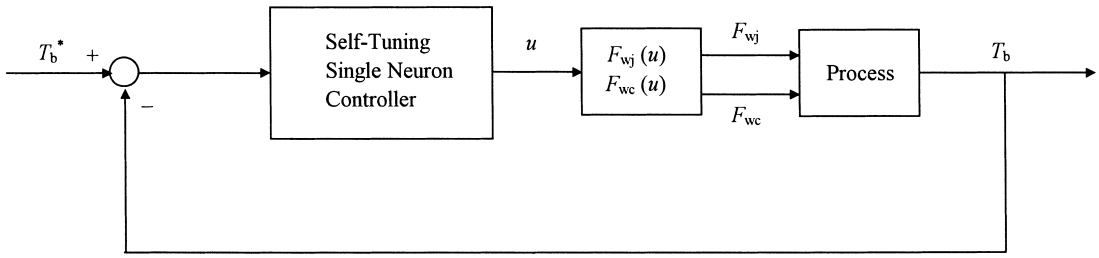

Fig. 4. Controller and process for the batch reactor.

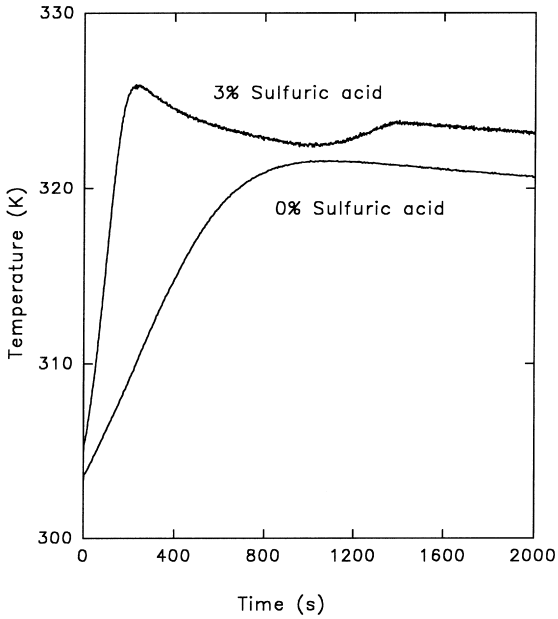

Fig. 5. Temperature profile of the adiabatic hydrolysis of acetic anhydride.

sulphuric acid (0%) and at an initial temperature of 32°C for a concentration of sulphuric acid of 3%. The time profile of temperature shown in Fig. 5 for the adiabatic reaction is quite steep, especially for the reaction loaded with 3% sulphuric acid. This highly exothermic hydrolysis reaction is a challenge for the proposed self-tuning single neuron controller in tracking a given trajectory. Similar results for the adiabatic hydrolysis of acetic anhydride can also be found in the report by Shukla and Pushpavanam [10].

6.2. Trajectory tracking for the hydrolysis of acetic anhydride

The performance of the self-tuning single neuron controller for trajectory tracking of different paths was investigated experimentally after a suitable choice of parameters c and b_{max} based on the performance test of the batch reactor control system loaded with water.

6.3. Water system

In determining suitable parameters c and b_{max} trajectory tracking of a stepwise-change isothermal path was carried out by the self-tuning single neuron controller in the batch reactor filled with water. Several test runs (Table 2) were performed for different combinations of parameters c and b_{max}. The parameters used for cases A, B and C (Table 2)

Table 2
Water test of the self-tuning single neuron controller in tracking a stepwise path

Case No.	Parameter c	b_{max}	No. of figure
A	1	10	6
B	3	10	7
C	3	20	8

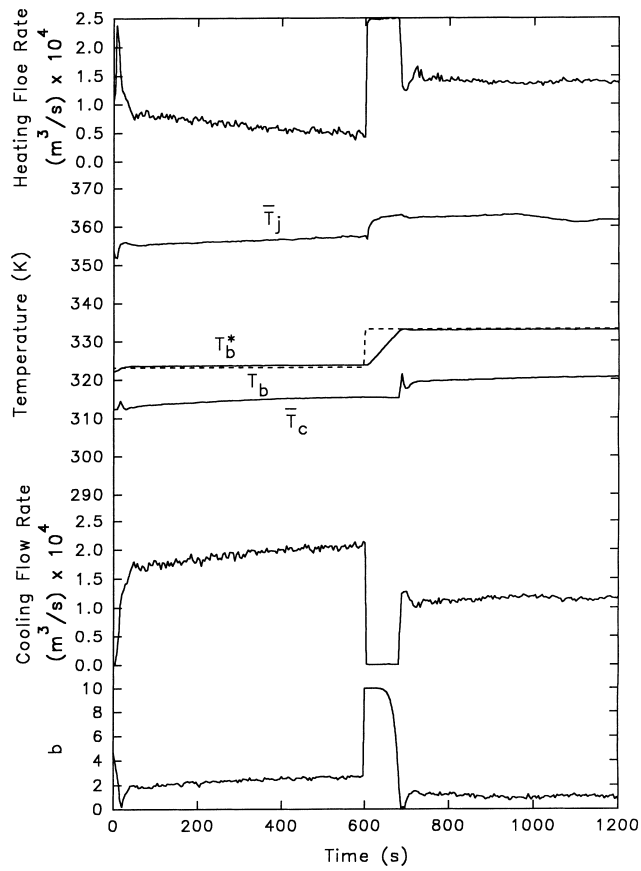

Fig. 6. Performance test of the self-tuning single neuron controller (case A of Table 2).

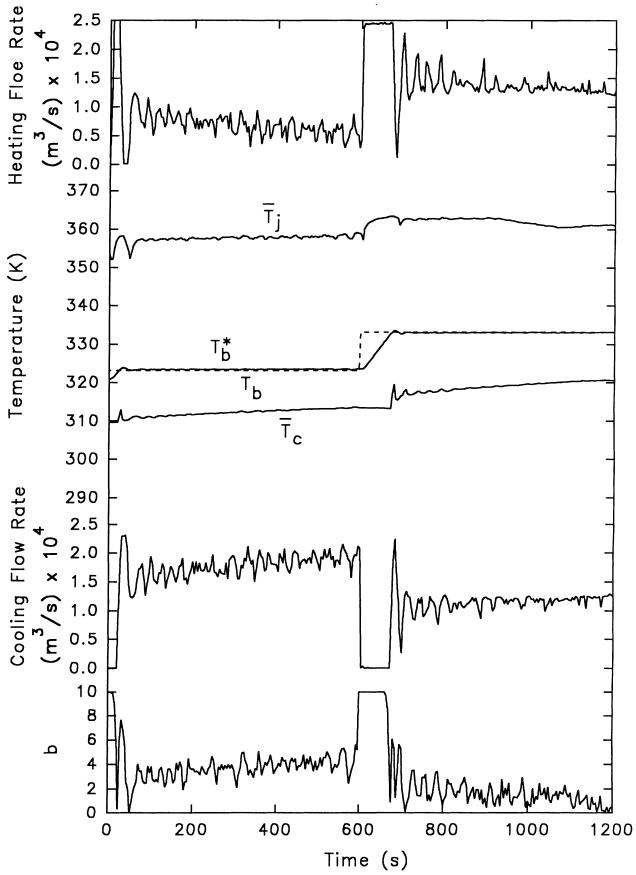

Fig. 7. Performance test of the self-tuning single neuron controller (case B of Table 2).

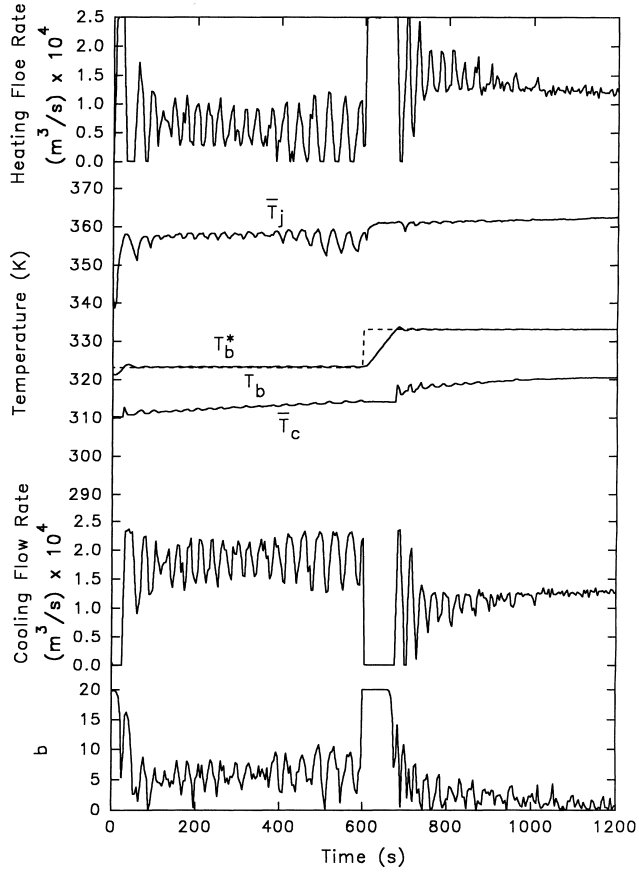

Fig. 8. Performance test of the self-tuning single neuron controller (case C of Table 2).

are acceptable based on the control performances presented in Figs. 6–8. Therefore, the parameter domain for this self-tuning single neuron controller seems to be quite large. In this parameter domain, we adopted parameters c and $b_{\max}$ to be 3 and 10 respectively for the following experiments. In the same plots (Figs. 6–8), the self-tuning function $b(t)$ is also shown. The effect of this self-tuning function is described below.

6.4. Hydrolysis of acetic anhydride

After testing the controller performance by adopting water as the reacting medium, we examined the self-tuning single neuron controller with the reaction system described in Section 3. As shown in Fig. 9, the following exponential path was tracked for the reacting medium loaded without sulphuric acid

$$T_b^*(t) = 348 - 28\exp(-t/1000)$$

Because a large reaction heat is involved at the initial stage of the reaction, the self-tuning single neuron controller responds appropriately and tight tracking of the trajectory can be obtained. The accompanying progression of pH and the variation of $b(t)$ are also shown in Fig. 9. Because the reacting medium was pumped out to the cooling and holding apparatus (Fig. 2), the temperature of the reacting medium was maintained at a near-isothermal condition (22–24°C) in the holding bottle. Therefore, the pH value of the reacting medium properly reflects the progression of the reaction. The variation of the pH value at the initial stage of the reaction ($t = 0$–200 s) signifies that the reaction is highly exothermic. At the later stage of the reaction ($t = 1600$–2000 s), no variation of pH can be detected, and total reaction can be inferred. In the same plot, the self-tuning function $b(t)$ of the single neuron controller reflects the control performance clearly. During the operation, if $e(t)$ deviates from zero, the self-tuning function $b(t)$ is increased. On the other hand, if $e(t)$ approaches zero, the self-tuning function $b(t)$ is decreased. One may argue that a fixed value of parameter b for the single neuron controller may still be workable; however, all the experiments performed in this work reveal that the observation of $b(t)$ points to the existence of a better domain of parameter b for the single neuron controller.

Next, experiments were performed to examine the applicability of the self-tuning single neuron controller when the reaction is carried out along an isothermal path. Satisfactory results are shown in Fig. 10. Furthermore, we tested the

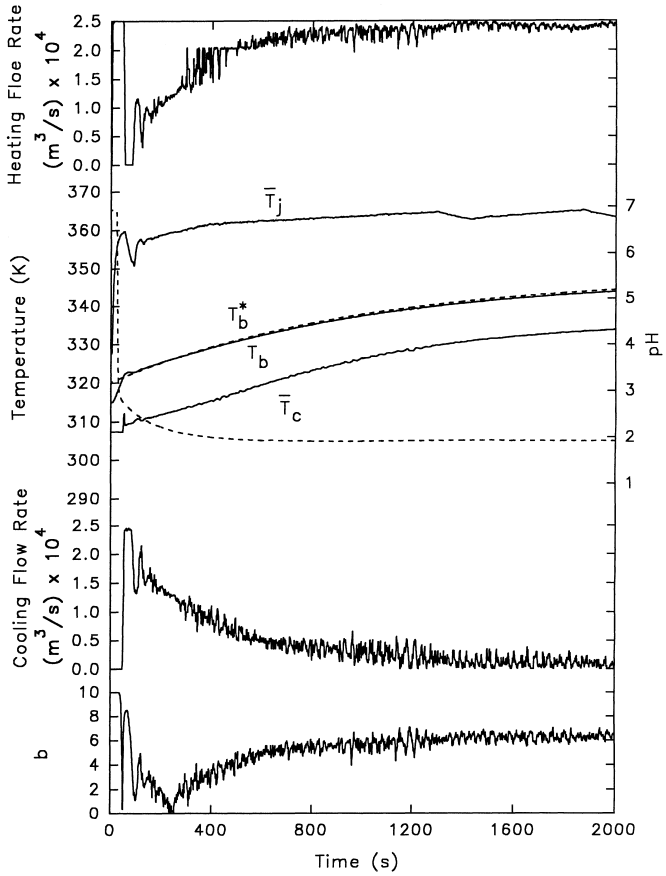

Fig. 9. Tracking of a first-order trajectory $T_b^*(t)$ (hydrolysis without catalyst).

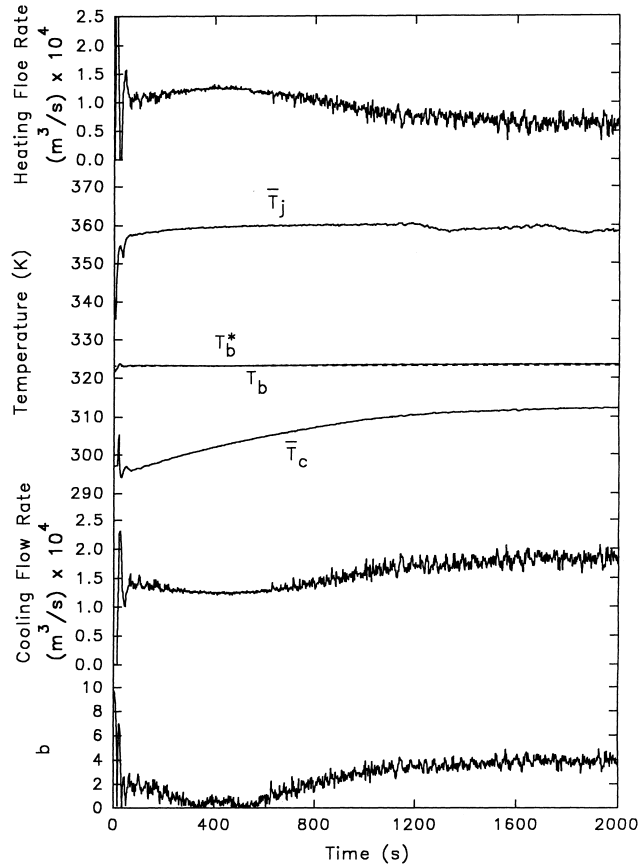

Fig. 10. Tracking of an isothermal trajectory $T_b^*(t)$ (hydrolysis without catalyst).

controller when the reaction was performed along a ramped, path followed by an isothermal path, as shown in Fig. 11. Fig. 11 demonstrates the applicability of the self-tuning single neuron controller for the successful tracking of trajectories in an exothermic chemical batch reactor without resorting to complicated mathematical manipulation involved in non-linear model-based controllers [3,4,7].

6.5. Sulphuric acid-catalysed hydrolysis of acetic anhydride

Finally, we tested the self-tuning single neuron controller by carrying out the reaction along a given trajectory. The reacting medium was loaded with 3% sulphuric acid initially. As shown in Fig. 5, the reaction rate was speeded up by the catalyst (sulphuric acid) at the initial stage of the reaction; to prevent the reaction from going out of control, water in V3 (8–10°C) was used as a coolant ($t = 0$–600 s). After that time (t>600 s), because the reaction was less intense, the coolant was switched from V3 to V1 (40°C). In this way, heating and cooling were balanced properly and the flow rates F_{wj} and F_{wc} were not bounded. The controller responded properly during the whole run, as shown in Fig. 12. The result of this experiment convinces us that the self-tuning single neuron controller is workable in a highly non-linear reaction system.

7. Conclusions

A self-tuning single neuron controller was applied in this work to tackle the temperature trajectory tracking problem in an exothermic chemical batch reactor. The performances of this controller were examined through simulation studies as well as experimental demonstrations. Only the experimental results are presented in this report. A suitable choice of parameters c and b_{max} can be easily obtained by testing the controller through a water test. The domain of each parameter is wide. Therefore, it is not difficult to determine parameters c and b_{max}.

On the basis of a suitable choice of parameters c and b_{max}, the self-tuning single neuron controller was tested by tracking given trajectories in reacting media loaded with or without sulphuric acid. When facing crucial conditions, this self-tuning single neuron controller performed satisfac-

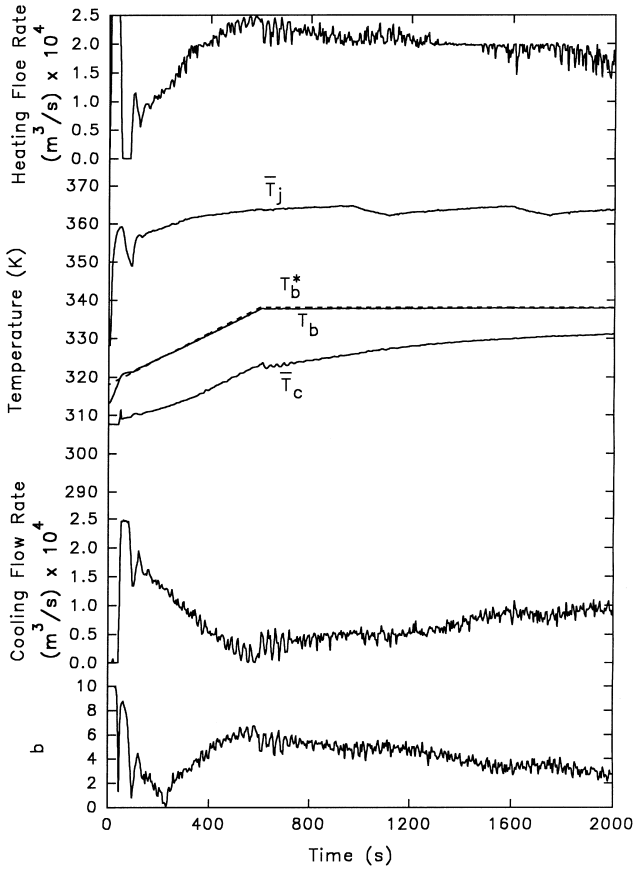

Fig. 11. Tracking of a ramped trajectory followed by an isothermal trajectory $T_b^*(t)$ (hydrolysis without catalyst).

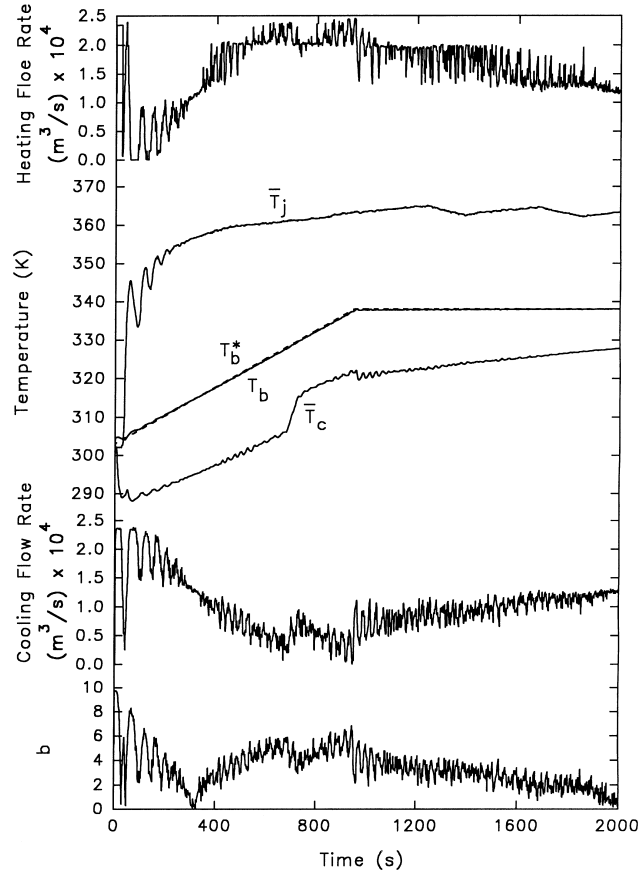

Fig. 12. Tracking of a ramped trajectory followed by an isothermal trajectory $T_b^*(t)$ (hydrolysis with 3% sulphuric acid as catalyst).

torily through experimental demonstrations. As the design equations for this controller are simple and can be implemented easily, it is recommended for practical application in the chemical industry.

8. Nomenclature

A	heat transfer area (m^2)
a	scaling factor used in Eq. (9)
a'	the saturated level of the NSF (Eq. (2))
b	parameter used in Eq. (9)
b'	the slope of the NSF (Eq. (2))
C	molar concentration of reagent (kmol m^{-3})
c	parameter in Eq. (11)
C_p	heat capacity (kJ kg^{-1})
CV	control valve
d	diameter of cooling coil (m)
D_{imp}	impeller diameter (m)
D_c	centreline diameter of internal coil helix (m)
D_j	outer diameter of annular jacket (m)
D_T	inner diameter of vessel (m)
E	primary element
E	sum of squared errors
e	input error signal
f	vector fields that characterize the state model
F	flow rate (m^3 s^{-3})
H	height of vessel (m)
$-\Delta H$	heat of reaction (kJ $kmol^{-1}$)
h	state/output map; non-linear saturated function (NSF)
I	indicator
k	the control step
L	length of coil (m)
N	agitator speed (rps)
N_c	number of coil turns
S	switch
t	time (s or min)
T	temperature (K or °C)
T	transmitter
$\bar{T}$	mean value of temperature measured at inlet and outlet (°C)
u	controller output
V	volume of reacting mixture (m^3)
V	vessel
x	vector of state variables
y	controlled output variable
Y	Relay

Greek symbols

η	learning rate
θ	threshold value
ρ	density (kg m^{-3})

Acronyms

A/D	analogue to digital
D/A	digital to analogue
NSF	the non-linear saturated function (Eq. (2))
RTD	resistance temperature detector
SSR	solid-state relay

Subscripts

*	desired
0	initial; inlet
b	batch side
c	cooling coil
i	inner
j	heating jacket
max	maximum
min	minimum
o	outer
w	water

Acknowledgements

We thank the National Science Council (NSC 86-2214-E-36-006) and Dr. T.S. Lin (President of Tatung Institute of Technology, Taipei, Taiwan) for all the support conducive to the completion of this work.

References

[1] C. Kravaris, R.A. Wright, J.F. Carrier, Comput. Chem. Eng. 13 (1989) 73.
[2] D.R. Lewin, R. Lavie, Ind. Eng. Chem. Res. 29 (1989) 89.
[3] C. Kravaris, C.B. Chung, AIChE J. 33 (1987) 592.
[4] J.S. Chang, K.L. Huang, Can. J. Chem. Eng. 72 (1994) 906.
[5] J.S. Chang, W.Y. Hseih, Ind. Eng. Chem. Res. 34 (1995) 545.
[6] J.S. Chang, S.T. Chung, J. Chin. Inst. Chem. Eng. 26 (1995) 213.
[7] J.S. Chang, J.S. Hsu, Y.T. Sung, Ind. Eng. Chem. Res. 35 (1996) 2247.
[8] C.T. Chen, W.D. Chang, C.I.Ch.E. Semiannual Meeting, Symposium On Process Control (1994) 63.
[9] J.S. Chang, Y.L. Liu, C.F. Ho, C.T. Chen, J. Chin. Inst. Chem. Eng. 28 (1996) 205.
[10] P.K. Shukla, S. Pushpavanam, Ind. Eng. Chem. Res. 33 (1994) 3202.
[11] D.P. Rao, S.K.B. Parey, Indian Chem. Eng. 30 (1988) 33.
[12] A. Jutan, E.S. Rodriguez II, Can. J. Chem. Eng. 65 (1987) 858.